

SUPPLEMENTAL MATERIAL

Methods

Sample information

Brachiopod shells were collected from the Peniche section (Lusitanian Basin, Portugal) in July, 2017. Altogether 62 specimens were selected for geochemical analyses, based on their good preservation and presence of intact calcite fibers in the secondary layer examined under a light microscope that were targeted in our analyses. 38 specimens were represented by rhynchonellids with impunctate shell structure (*Gibbirhynchia*, *Nannirhynchia*, *Soaersirhynchia*, *Tetrarhynchia*, *Prionorhynchia*, *Pseudogibbirhynchia*, and one unidentified rhynchonellid), 9 specimens by terebratulids (*Lobothyris*, *Zeilleria*, and *Aulacothyris*) with punctate shell structure, 14 specimens by the punctate spiriferinid *Liospiriferina*, and one sample by the impunctate koninckinid (athyridid) (*Konickella*).

Sample preparation and geochemical analyses

For all samples, physical cleaning and powder collection were done under a binocular microscope. First, samples were carefully cleaned on the surface, removing adhering sediments with a handheld precision driller (Proxxon) mounted with an abrasion head. The external surface of the shell was gently scraped with a razorblade in order to remove the primary layer, which is considered not to crystallize in equilibrium with seawater (Carpenter & Lohmann, 1995; Rollion-Bard et al., 2019). Approximately 1-5 mg of homogenous powder was then collected from 62 specimens with a carbide pen. About 40-100 µg of powder from each specimen was analyzed for carbon and oxygen isotopes on isotope-ratio mass spectrometer (IRMS) MAT253 coupled with semi-automated carbonate preparation device Kiel IV (Thermo Scientific) at the geochemical laboratory of the Slovak Academy of Sciences in Banská Bystrica. Isotope composition was

measured against CO₂ reference gas and raw values were calibrated using international reference material NBS18 and two working standards with $\delta^{13}\text{C}$ of 5.014‰, 2.48‰ and 9.30‰, and $\delta^{18}\text{O}$ of -23.2‰, -2.40 and -15.30‰, respectively. All the values are reported as per mille vs. VPDB, and the typical uncertainty for a measurement was 0.02‰ for $\delta^{13}\text{C}$ and 0.04‰ for $\delta^{18}\text{O}$. The remaining geochemical analyses – major and trace element concentration, boron and radiogenic strontium isotope analyses were carried out at GEOMAR Helmholtz Centre for Ocean Research Kiel, Germany. Detailed description of the laboratory protocols is available in Jurikova et al. (2019) and Krabbenhöft et al. (2009). Altogether 55 samples (out of the total of 62) were measured for elemental concentrations, out of which, 42 had sufficient boron content (minimum 15 ng per sample was required) and were then further processed for boron isotope analyses. Briefly, approximately 1-5 mg of homogenous calcite powder of each specimen was repeatedly rinsed in MQ and ethanol to clean from any potential fine particulate contamination (clays), oxidized to remove residual organics, and finally dissolved in 0.5 M HNO₃. A 10% aliquot of each sample was measured for major and trace element content using a Quadrupole ICP-MS (Agilent 7500x). The reproducibility was better than 3% for B/Ca, Mg/Ca and Sr/Ca, and better than 10% for Al/Ca and Mn/Ca assessed by repeated measurements of carbonate reference materials JCp-1, JCT-1 and an in-house brachiopod standard MVS-1. Boron was separated on micro-columns using Amberlite IRA 743 resin and isotope ratios determined on a Thermo Scientific Neptune Plus MC-ICP-MS. The analytical reproducibility on $\delta^{11}\text{B}$ was assessed by measurements of carbonate reference materials along with samples; for the international coral standard JCp-1 $\delta^{11}\text{B} = 24.24 \pm 0.16\text{‰}$ (2SD, n = 2), and for our in-house brachiopod standard MVS-1 $\delta^{11}\text{B} = 15.85 \pm 0.11\text{‰}$ (2SD, n = 2). The $\delta^{11}\text{B}$ of NIST RM 8301 Coral and NIST RM 8301 Foraminifera was $24.22 \pm 0.10\text{‰}$ and $14.55 \pm 0.16\text{‰}$ (2SD, n = 1), respectively. The long-term reproducibility on $\delta^{11}\text{B}$ was better than $\pm 0.20\text{‰}$ assessed by repeated measurements of JCp-

1; $\delta^{11}\text{B} = 24.41 \pm 0.18\%$ (2SD (standard deviation); $n = 15$), and the total procedural blank was for all samples <100 pg ($<0.1\%$ of the sample size, $n = 12$; Jurikova et al., 2019).

To further assess the degree of preservation, and to expand the age model to the upper Pliensbachian, selected samples were additionally analyzed for $^{87}\text{Sr}/^{86}\text{Sr}$ in order to compare the independent and robust biostratigraphic identification with Sr isotope stratigraphy (SIS) age estimates as alteration sensitive monitor. Sr was extracted using Sr-spec ion chromatography and measured using a ThermoFisher TRITON TIMS. All generated $^{87}\text{Sr}/^{86}\text{Sr}$ were normalized to the accepted NIST SRM 987 $^{87}\text{Sr}/^{86}\text{Sr}$ of 0.710248. The whole procedural reproducibility was determined on brachiopod sample 876-17 via two complete replicates prepared throughout two individual runs with different sample sizes (by a factor of 2). Each replicate was measured three times (hence $n = 6$), with a 2SD of 0.000006, to be better than mean 2 SE (standard error) of individual measurements on 876-17 (mean 2SE: 0.000009) and NIST-SRM-987 of 4 sessions related to this data set (2SE: 0.000005, $n = 13$). Given the high level of reproducibility the individual uncertainties of the measurements are displayed. As a conservative assumption usually an uncertainty of 0.000015 needs to be applied as still sufficient diagnostic. A whole procedural blank of <0.02 ng at mean separated Sr aliquot of 106 ng per sample (range: 48 to 226 ng) was sufficiently low and no correction was required.

For the whole data set and uncertainties of individual boron and strontium isotopes and element ratios see Table S1.xlsx.

Age model

The age model was constructed by using 405 kyr long eccentricity cycles discriminated by Huang & Hesselbo (2014) based on their bulk carbonate carbon isotope record, for the interval between -2.31 and 38.5 meters in the Peniche Section (following the stratigraphic log and scales

from Hesselbo et al., 2007). Along this interval six long eccentricity cycle can be distinguished (approximate cycle intervals: -2.3 to 4.6 m; 4.6–9.8 m; 9.8–16.3 m; 16.3–23.3 m; 23.3–31.7 m; 31.7–38.5 m). Within each cycle, sedimentation rate was considered constant since there is no evidence of any significant stratigraphic gaps. After constraining the duration of the cycles an interpolation of age could be made between the lower and upper end of each cycles and assigned to every centimeter. By assuming the age of 183.7 ± 0.5 Ma (Ogg et al., 2016) to the Pliensbachian/Toarcian boundary (located at -32 cm on our stratigraphic log), the ages derived from cyclostratigraphy could be transformed to absolute ages. The age model for the lowermost part of the section between -2.3 and -14.4 m (upper Margaritatus and the Spinatum ammonite zones) is based on Sr isotope stratigraphy, assuming a linear $^{87}\text{Sr}/^{86}\text{Sr}$ -age relationship (McArthur et al., 2016). Between the well-fitting (SIS) sample P3 (at -13.45 m, upper Margaritatus Zone) having the lowermost stratigraphic position and the last known age data from cyclostratigraphic estimation, an interpolation was made to expand our age model.

Determination of seawater $\delta^{11}\text{B}$ and pH calibration

In seawater, boron occurs in two species: as borate ion $[\text{B}(\text{OH})_4^-]$ and boric acid $[\text{B}(\text{OH})_3]$ with a constant fractionation between these two (Klochko et al., 2006). The relative proportions of boron species as well as their isotopic compositions are a function of pH. Upon precipitation of calcium carbonate, the borate ion is preferentially incorporated into marine calcifiers (Sanyal et al., 2000), the composition of which can be used to constrain the seawater pH, providing the $\delta^{11}\text{B}$ value of ambient seawater is known.

Boron has a residence time of 11-20 million years in the ocean (Lemarchand et al., 2002). While homogenous in the ocean at any point in time, bulk seawater $\delta^{11}\text{B}$ hence varies on multi-

million-year timescales. Joachimski et al. (2005) provided a first reconstruction of Phanerozoic seawater $\delta^{11}\text{B}$. Their modelling approach throughout the Phanerozoic based on Late Jurassic and Permian brachiopod data, but leaving Early Jurassic values to model prediction, proposed relatively high seawater $\delta^{11}\text{B}$ values for the latest Pliensbachian (~40–42‰). These values are, however, too high to quantify pH from our measured $\delta^{11}\text{B}$ values and result beyond the effective proxy range when applying any of the currently available $\delta^{11}\text{B}$ -pH calibrations (Lécuyer et al., 2002; Penman et al., 2013; Jurikova et al., 2019).

A Phanerozoic $p\text{CO}_2$ modeling (based on proxy records of stomatal indices and paleosols from Royer et al. 2004) study by Ridgwell (2005), which considers carbonate production dominantly neritic in style (as it was prevailing in the Early Jurassic), provided a pH model, with a relatively large scatter for the Early Jurassic (with a minimum pH value of 7.4 and maximum of 7.9), due to the uncertainties on the atmospheric $p\text{CO}_2$ estimates. A mean value of 7.7 at 183 Ma (latest Pliensbachian) can be computed. Considering the environmental conditions during the Early Jurassic as a high- $p\text{CO}_2$ world, a mean seawater pH below the present-day conditions seems reasonable. By applying the 7.7 initial pH value and the pH dependency of boron incorporation into brachiopod shell using the calibration equation for brachiopods of Lécuyer et al. (2002), the empirical boron isotope equilibrium constant provided by Klochko et al. (2006), and a boric acid dissociation constant calculated following Dickson (1990), this approach results in a seawater $\delta^{11}\text{B}$ value of 36.55‰. This value thus appears to present the most optimal choice, and allows the full expression of the proxy and was used for our pH reconstructions.

The following calibration equation provided by Lécuyer et al. (2002) was used:

$$\text{pH} = -\log \left(\frac{0.023}{\frac{\delta^{11}\text{B}_{brachiopod} + 1000}{\delta^{11}\text{B}_{seawater} + 1000} - 0.976} - {}^{11-10}K_B \right) + pK_B$$

Where the constants 0.023 and 0.976 were empirically derived from $\delta^{11}\text{B}$ composition of brachiopod calcite (Lécuyer et al., 2002), $^{11-10}K_B = 1.0272$ representing the boron isotope equilibrium constant (Klochko et al., 2006) and $\text{p}K_B = 8.63$ is the dissociation constant for boric acid (Dickson et al., 1990) based on $T = 20^\circ\text{C}$ and salinity = 40 (salinity units; Early Jurassic value according to Hay et al., 2006). In addition to the calibration provided by Lécuyer et al. (2002), which considers a biological effect on boron isotope fractionation in brachiopod shells, we further provide pH calculations based on the empirical inorganic boron isotope fractionation derived by Klochko et al. (2006), applying the equation:

$$\text{pH} = \text{p}K_B - \log \left(\frac{\delta^{11}B_{\text{seawater}} - \delta^{11}B_{\text{borate}}}{\delta^{11}B_{\text{seawater}} - ^{11-10}K_B \delta^{11}B_{\text{borate}} - 1000X(^{11-10}K_B - 1)} \right)$$

Following the same procedure as described above, a retrospective calculation of seawater $\delta^{11}\text{B}$ using the inorganic borate ion to pH relationship (Klochko et al., 2006) and assuming a present pH of 7.7 yields a seawater value of 38.86%.

Temperature reconstruction

Seawater temperatures were derived from brachiopod $\delta^{18}\text{O}$ data based on the equation of Anderson and Arthur (1983), assuming that the seawater $\delta^{18}\text{O} = -1\text{‰}$ (VSMOW) for an ice free world. In order to illustrate the sensitivity of our temperature calibration to seawater $\delta^{18}\text{O}$, an error envelope has been added to Fig. 2B and Fig S2B where the two end members are based on seawater values of -2 and 0‰. This envelope, also accounts for sensitivities of seawater $\delta^{18}\text{O}$ to salinity change, since under subtropical climate a 1‰ decrease in seawater $\delta^{18}\text{O}$ is equal to 2.5 ppt decrease in salinity (Lusitanian Basin was located at the southern margin of the subtropical

climate belt in the Early Jurassic (Mattioli et al., 2008)) (Craig and Gordon, 1965; Lécuyer et al., 2003).

Modeling of seawater alkalinity, $p\text{CO}_2$, aragonite and calcite saturation state

Modeling of seawater parameters was performed in the software environment R applying the seawater carbonate chemistry package “seacarb” of Gattuso et al. (2019). First, to compute alkalinity, salinity was assumed to be 40 (estimation of Hay et al., 2006 for the Early Jurassic), ambient temperature was based on our brachiopod $\delta^{18}\text{O}$ -derived temperature data, $p\text{CO}_2$ is derived from stomatal index from Steinthorsdottir and Vajda (2015) and McElwain et al. (2005), and pH is based on brachiopod $\delta^{11}\text{B}$. This approach also provides temporal variability to our modeled seawater parameters. Second, due to differences in the stratigraphic resolution between the $\delta^{11}\text{B}$ -pH and the published $p\text{CO}_2$ records, we have averaged the empirical $p\text{CO}_2$ data and modeled alkalinity to six coarser stratigraphic intervals. These averaged intervals are the following: upper Pliensbachian; lower Polymorphum (\approx Tenuicostatum) Zone; upper Polymorphum Zone; lower Levisoni (\approx Falciferum) Zone; middle Levisoni Zone; upper Levisoni Zone. On the basis of alkalinity and pH a stratigraphically-refined $p\text{CO}_2$ estimation was made, providing bed-scale resolution for the record. Subsequently, the ocean calcite and aragonite saturation states (Ω) were reconstructed, determined with the use of $p\text{CO}_2$, pH, and temperature as input parameters. For an uncertainty envelope from each input parameters the maximum and minimum values were taken from the averaged stratigraphic intervals and upper and lower estimates for $p\text{CO}_2$, alkalinity, aragonite and calcite saturation were made. All parameters were computed with both $\delta^{11}\text{B}$ -pH calibration scenarios ((1) brachiopod-specific $\delta^{11}\text{B}$ incorporation (Lécuyer et al., 2002) or (2) inorganic $\delta^{11}\text{B}_{\text{cc}}$ to $\delta^{11}\text{B}_{\text{borate ion}}$ relationship (Klochko et al., 2006)).

Therefore: $ALK1$, Ω_{calcite} and $\Omega_{\text{aragonite}}$ are based on pH scenario 1; $ALK2$, Ω_{calcite} and $\Omega_{\text{aragonite}}$ are based on pH scenario 2; for the pCO_2 Fig. 2 illustrates the record following scenario 1 while Fig. S2 follows scenario 2. The modeled changes in alkalinity and in calcite and aragonite saturation states are shown in Fig. S4.

Species-specific effects

Exclusive collection of single species or at a consentaneous higher taxonomic level along the entire Peniche section was not possible due to the nature of stratigraphic appearance of brachiopods (see Comas-Rengifo et al., 2015). Furthermore, the interval of the uppermost Polymorphum and lower Levisoni Zones are extremely scarce in brachiopods (see Suan et al., 2008, Comas-Rengifo et al., 2015).

Although $\delta^{11}B$ values may be potentially affected by species-specific fractionation effects, the major shift in $\delta^{11}B$ from $\sim 13.75\text{‰}$ in the lower parts of the Polymorphum Zone to $12.1\text{--}12.5\text{‰}$ in the upper parts of the Polymorphum Zone, is exhibited by single species; the rhynchonellid *Nannirhynchia pygmaea*. This species went extinct at the Polymorphum/Levisoni boundary and thus cannot be sampled in the higher parts of the section. At higher stratigraphic levels, where bioturbation is more limited, (with *Zoophycos* that does not generate intense mixing of shells) $\delta^{11}B$ values differ between species by less than $<0.5\text{‰}$ (Fig S4). Beds 974 and 981 are strongly bioturbated and are typical of the Spinatum Zone prior to the end-Pliensbachian/Toarcian $\delta^{13}C$ anomaly. At these horizons, the offsets between two co-occurring species exceed $>1\text{‰}$; however, given the extensive *Thalassinoides* bioturbation, we posit that the brachiopods may not be contemporaneous, but rather of mixed age on the scale of over several thousands of years. Therefore, burrowing complicates the discrimination of species-specific effects vs. changes in seawater carbonate chemistry.

Elemental ratios and preservation

The concentration of different elements and particularly Mn/Ca and Sr/Ca ratios indicate a good preservation of our analyzed brachiopod shells, without any obvious relationship between sedimentary facies (limestones and marls) and element/Ca ratios (Fig. S1). The Sr/Ca and Mn/Ca values were within the range of well-preserved brachiopods (Sr/Ca: ~0.4–2 mmol/mol and Mn/Ca: <0.46 mmol/mol, Fig. S1G; Brand et al., 2003; Korte et al., 2008). The lack of notable co-variations between Al/Ca and $\delta^{11}\text{B}$ suggests that any potential presence of clay minerals had a negligible effect on the recorded $\delta^{11}\text{B}$ values (Fig. S1B). Two samples showed anomalously high Mn/Ca values and were excluded from the study (Samples: P43 0.55 mmol/mol and P49 0.97 mmol/mol). The sample with the highest Mn/Ca value was not analyzed for $\delta^{11}\text{B}$ and was excluded thereafter. The second sample with the high Mn/Ca ratio was further characterized by relatively high Al/Ca, the highest Mg/Ca and low B/Ca values, suggesting a substantial diagenetic overprint (Fig. S1A; C; D). Both samples were hence considered as overprinted, leaving altogether 41 samples for our $\delta^{11}\text{B}$ interpretations.

Some brachiopods showed $^{87}\text{Sr}/^{86}\text{Sr}$ values that were more radiogenic than those expected for the marine environment during the late Pliensbachian–early Toarcian (McArthur et al., 2000; McArthur et al., 2016; McArthur et al., 2019). Considering the strong sensitivity of the strontium isotope system to diagenesis (Veizer & Compston, 1974; Shields et al. 2003; Korte and Ullmann, 2016) and the fact that late Pliensbachian – early Toarcian seawater was one of the most depleted in radiogenic strontium, even a very minor alteration of the original composition could trigger the observed offset. The offset between the expected and measured $^{87}\text{Sr}/^{86}\text{Sr}$ values does not show

any systematic relationship with $\delta^{11}\text{B}$ values (Fig. S1H; I) suggesting that, if caused by minor diagenetic effects, these did not notably impact the Peniche $\delta^{11}\text{B}$ brachiopod record. We note that the Sr isotope ratios are more sensitive to alterations than $\delta^{11}\text{B}$ and could therefore be regarded as a highly reliable indicator for sufficient preservation especially in cases of matching biostratigraphy with SIS. In addition, the recent, mostly belemnite-based study by McArthur et al. (2019) suggests excellent preservation of seawater $^{87}\text{Sr}/^{86}\text{Sr}$ signal for the early Toarcian, implying that post-depositional diagenesis did not have a significant effect in Peniche. Furthermore, there was no relationship between the recorded $\delta^{11}\text{B}$ values and the taxonomy of the analyzed brachiopods, suggesting no significant taxonomic control on the $\delta^{11}\text{B}$ record. Mg/Ca ratio values in brachiopods are highly variable among different taxonomic groups (Ullmann et al., 2017) and the observed lack of any notable relationship between $\delta^{11}\text{B}$ and Mg/Ca could further lend support for a negligible taxonomic effect on our Lower Jurassic boron isotope record (Fig. S1D).

REFERENCES

- Anderson, T. F., and Arthur, M. A., 1983. Stable isotopes of oxygen and carbon and their application to sedimentological and paleoenvironmental problems, in Arthur, M. A., and others, eds.. Stable isotopes in sedimentary geology: Society of Economic Paleontologists and Mineralogists, Short Course No. 10, p. 1-1-1-151.
- Brand, U., Logan, A., Hiller, N. and Richardson, J., 2003. Geochemistry of modern brachiopods: applications and implications for oceanography and paleoceanography. *Chemical Geology*, 198(3-4), pp.305-334.

- Carpenter, S.J. and Lohmann, K.C., 1995. $\delta^{18}\text{O}$ and $\delta^{13}\text{C}$ values of modern brachiopod shells. *Geochimica et Cosmochimica Acta*, 59(18), pp.3749-3764
- Comas-Rengifo, M.J., Duarte, L.V., Felix, F.F., Joral, F.G., Goy, A. and Rocha, R.B., 2015. Latest Pliensbachian-Early Toarcian brachiopod assemblages from the Peniche section (Portugal) and their correlation. *Episodes*, 38(1), pp.2-8.
- Craig, H., & Gordon, L. I., 1965. Deuterium and oxygen 18 variations in the ocean and the marine atmosphere, in *Stable Isotopes in Oceanographic Studies and Paleotemperatures*, edited by E. Tongiorgi, pp. 9 – 130, Spoleto, Cons. Naz. delle Ric., Lab. di Geol. Nucl., Pisa, Italy
- Dickson, A.G., 1990. Thermodynamics of the dissociation of boric acid in synthetic seawater from 273.15 to 318.15 K. *Deep Sea Research Part A. Oceanographic Research Papers*, 37(5), pp.755-766.
- Gattuso, J.P., 2019. seacarb: Seawater Carbonate Chemistry with R. R package version 3.2.12. CRAN.R-project.org/package=seacarb
- Hay, W.W., Migdisov, A., Balukhovskiy, A.N., Wold, C.N., Flögel, S. and Söding, E., 2006. Evaporites and the salinity of the ocean during the Phanerozoic: Implications for climate, ocean circulation and life. *Palaeogeography, Palaeoclimatology, Palaeoecology*, 240(1-2), pp.3-46.
- Hesselbo, S.P., Jenkyns, H.C., Duarte, L.V. and Oliveira, L.C., 2007. Carbon-isotope record of the Early Jurassic (Toarcian) Oceanic Anoxic Event from fossil wood and marine carbonate (Lusitanian Basin, Portugal). *Earth and Planetary Science Letters*, 253(3-4), pp.455-470.
- Huang, C. and Hesselbo, S.P., 2014. Pacing of the Toarcian Oceanic Anoxic Event (Early Jurassic) from astronomical correlation of marine sections. *Gondwana Research*, 25(4), pp.1348-1356.

- Joachimski, M.M., Simon, L., Van Geldern, R. and Lécuyer, C., 2005. Boron isotope geochemistry of Paleozoic brachiopod calcite: implications for a secular change in the boron isotope geochemistry of seawater over the Phanerozoic. *Geochimica et Cosmochimica Acta*, 69(16), pp.4035-4044.
- Jurikova, H., Liebetrau, V., Gutjahr, M., Rollion-Bard, C., Hu, M.Y., Krause, S., Henkel, D., Hiebenthal, C., Schmidt, M., Laudien, J. and Eisenhauer, A., 2019. Boron isotope systematics of cultured brachiopods: response to acidification, vital effects and implications for palaeo-pH reconstruction. *Geochimica et Cosmochimica Acta*, 248, pp.370-386.
- Klochko, K., Kaufman, A.J., Yao, W., Byrne, R.H. and Tossell, J.A., 2006. Experimental measurement of boron isotope fractionation in seawater. *Earth and Planetary Science Letters*, 248(1-2), pp.276-285.
- Korte, C., Jones, P.J., Brand, U., Mertmann, D. and Veizer, J., 2008. Oxygen isotope values from high-latitudes: Clues for Permian sea-surface temperature gradients and Late Palaeozoic deglaciation. *Palaeogeography, Palaeoclimatology, Palaeoecology*, 269(1-2), pp.1-16.
- Korte, C. and Ullmann, C.V., 2016. Permian strontium isotope stratigraphy. Geological Society, London, Special Publications, 450, pp.SP450-5.
- Krabbenhöft, A., Fietzke, J., Eisenhauer, A., Liebetrau, V., Böhm, F. and Vollstaedt, H., 2009. Determination of radiogenic and stable strontium isotope ratios ($^{87}\text{Sr}/^{86}\text{Sr}$; $\delta^{88/86}\text{Sr}$) by thermal ionization mass spectrometry applying an $^{87}\text{Sr}/^{84}\text{Sr}$ double spike. *Journal of Analytical Atomic Spectrometry*, 24(9), pp.1267-1271.
- Lécuyer, C., Grandjean, P., Reynard, B., Albarede, F. and Telouk, P., 2002. $^{11}\text{B}/^{10}\text{B}$ analysis of geological materials by ICP-MS Plasma 54: application to the boron fractionation between brachiopod calcite and seawater. *Chemical Geology*, 186(1-2), pp.45-55.

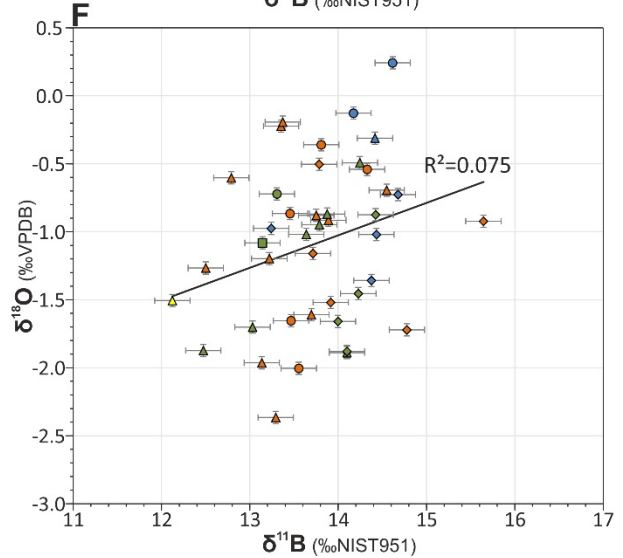
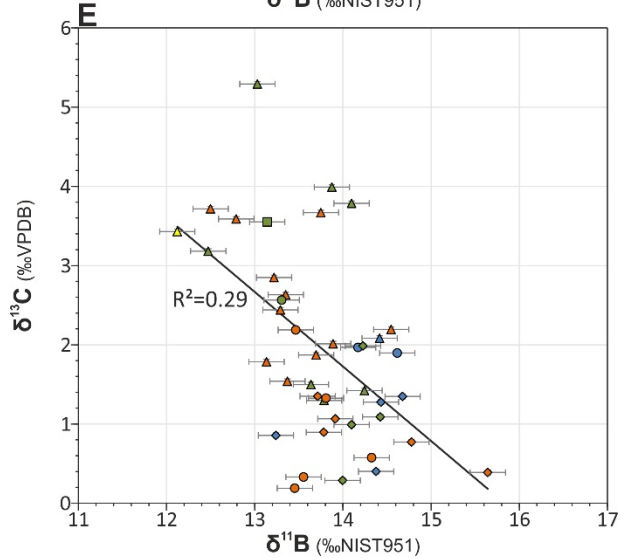
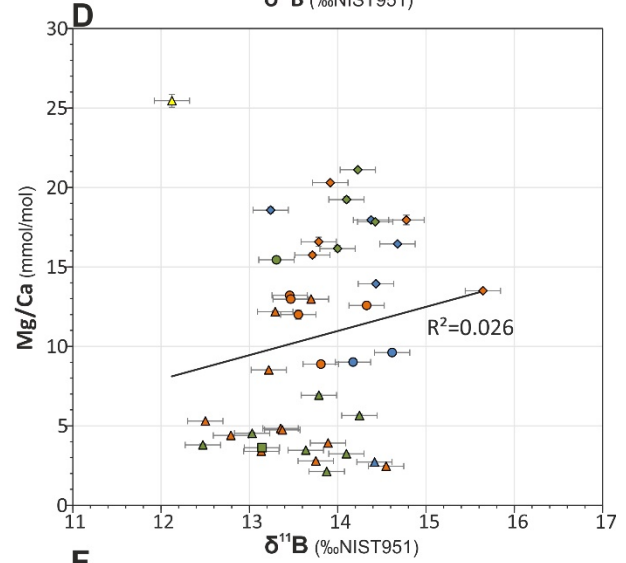
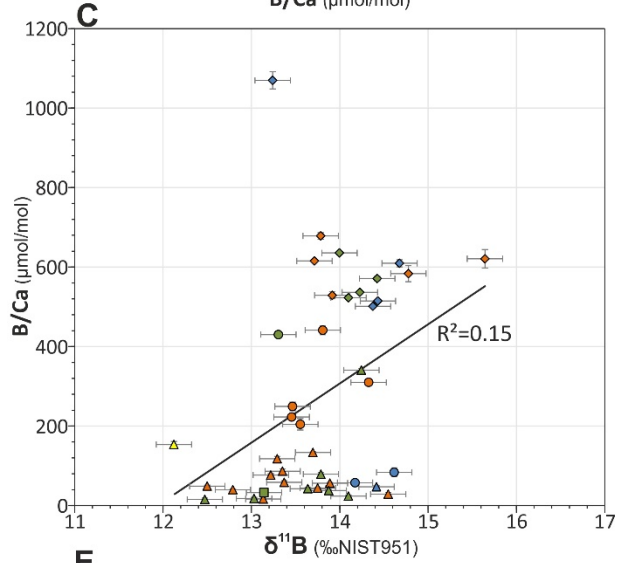
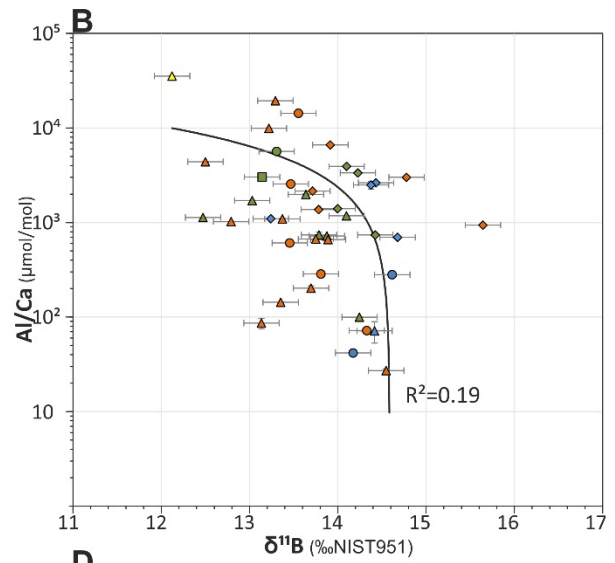
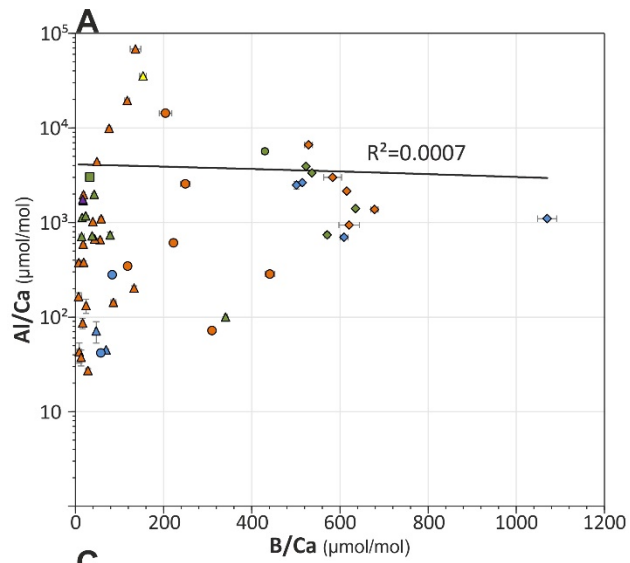
- Lécuyer, C., Picard, S., Garcia, J.P., Sheppard, S.M., Grandjean, P. and Dromart, G., 2003. Thermal evolution of Tethyan surface waters during the Middle-Late Jurassic: Evidence from $\delta^{18}\text{O}$ values of marine fish teeth. *Paleoceanography*, 18(3).
- Lemarchand, D., Gaillardet, J., Lewin, E. and Allegre, C.J., 2002. Boron isotope systematics in large rivers: implications for the marine boron budget and paleo-pH reconstruction over the Cenozoic. *Chemical Geology*, 190(1-4), pp.123-140.
- Mattioli, E., Pittet, B., Suan, G., Mailliot, S., 2008. Calcareous nannoplankton changes across the early Toarcian oceanic anoxic event in the western Tethys. *Paleoceanography*, 23(3).
- McArthur, J.M., Donovan, D.T., Thirlwall, M.F., Fouke, B.W. and Matthey, D., 2000. Strontium isotope profile of the early Toarcian (Jurassic) oceanic anoxic event, the duration of ammonite biozones, and belemnite palaeotemperatures. *Earth and Planetary Science Letters*, 179(2), pp.269-285.
- McArthur, J.M., Steuber, T., Page, K.N. and Landman, N.H., 2016. Sr-isotope stratigraphy: assigning time in the Campanian, Pliensbachian, Toarcian, and Valanginian. *The Journal of Geology*, 124(5), pp.569-586.
- McArthur, J.M., Page, K., Duarte, L. V., Thirlwall, M. F., Li, Q.; Weis, R., and Comas-Rengifo, M. J., 2019. Sr-isotope stratigraphy ($^{87}\text{Sr}/^{86}\text{Sr}$) of the lowermost Toarcian of Peniche, Portugal, and its relation to ammonite zonations. *Newsletters on Stratigraphy, ACE*, 15(16), 14 doi: 10.1127/nos/2019/0492
- McElwain, J.C., Wade-Murphy, J. and Hesselbo, S.P., 2005. Changes in carbon dioxide during an oceanic anoxic event linked to intrusion into Gondwana coals. *Nature*, 435(7041), p.479.
- Ogg, J.G., Ogg, G. and Gradstein, F.M., 2016. A concise geologic time scale: 2016. Elsevier, pp. 234

- Penman, D.E., Hönisch, B., Rasbury, E.T., Hemming, N.G. and Spero, H.J., 2013. Boron, carbon, and oxygen isotopic composition of brachiopod shells: Intra-shell variability, controls, and potential as a paleo-pH recorder. *Chemical Geology*, 340, pp.32-39.
- Ridgwell, A., 2005. A Mid Mesozoic Revolution in the regulation of ocean chemistry. *Marine Geology*, 217(3-4), pp.339-357.
- Rollion-Bard C., Milner García S., Burckel P., Angiolini L., Jurikova H., Tomašových A., Henkel D. Assessing the biomineralization processes in the shell layers of modern brachiopods from oxygen isotopic composition and elemental ratios: Implication for their use as paleoenvironmental proxies. *Chemical Geology*, 524, pp.49-66.
- Royer, D.L., Berner, R.A., Montañez, I.P., Tabor, N.J. and Beerling, D.J., 2004. CO₂ as a primary driver of phanerozoic climate. *GSA today*, 14(3), pp.4-10.
- Sanyal, A., Nugent, M., Reeder, R.J. and Bijma, J., 2000. Seawater pH control on the boron isotopic composition of calcite: evidence from inorganic calcite precipitation experiments. *Geochimica et Cosmochimica Acta*, 64(9), pp.1551-1555.
- Shields, G.A., Carden, G.A., Veizer, J., Meidla, T., Rong, J.Y. and Li, R.Y., 2003. Sr, C, and O isotope geochemistry of Ordovician brachiopods: a major isotopic event around the Middle-Late Ordovician transition. *Geochimica et Cosmochimica Acta*, 67(11), pp.2005-2025.
- Steinthorsdottir, M. and Vajda, V., 2015. Early Jurassic (late Pliensbachian) CO₂ concentrations based on stomatal analysis of fossil conifer leaves from eastern Australia. *Gondwana Research*, 27(3), pp.932-939.
- Suan, G., Mattioli, E., Pittet, B., Mailliot, S. and Lécuyer, C., 2008. Evidence for major environmental perturbation prior to and during the Toarcian (Early Jurassic) oceanic anoxic event from the Lusitanian Basin, Portugal. *Paleoceanography*, 23(1).

Ullmann, C.V., Frei, R., Korte, C. and Lüter, C., 2017. Element/Ca, C and O isotope ratios in modern brachiopods: Species-specific signals of biomineralization. *Chemical Geology*, 460, pp.15-24.

Veizer, J. and Compston, W., 1974. $^{87}\text{Sr}/^{86}\text{Sr}$ composition of seawater during the Phanerozoic. *Geochimica et Cosmochimica Acta*, 38(9), pp.1461-1484.

FIGURE CAPTIONS



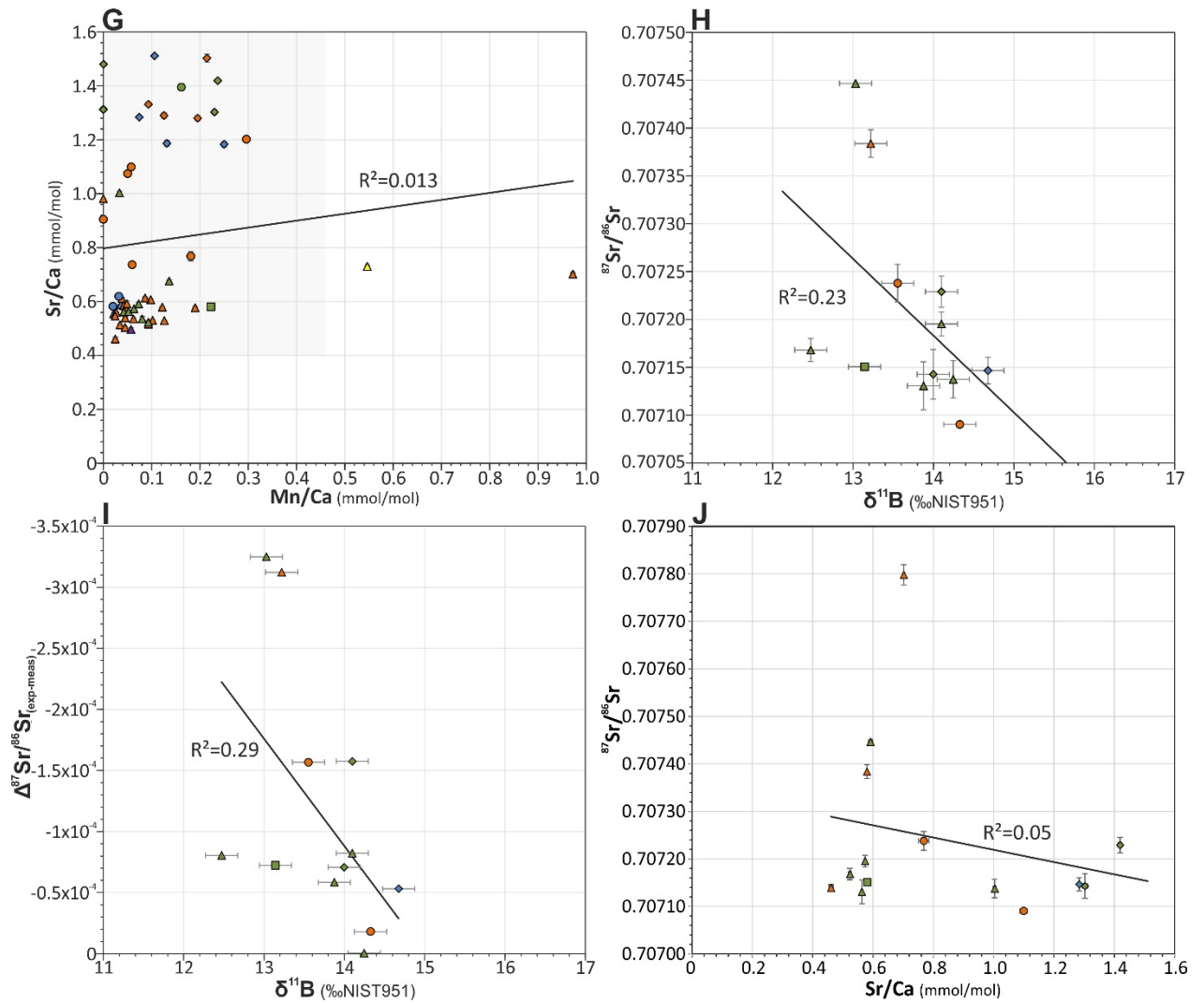


Figure S1. Element/Ca ratios and isotope data cross-plots of Pliensbachian-Toarcian brachiopods. Symbols denote brachiopod groups on order level: triangle: Rhyconellids; circle: Terebratulids; diamond: Spiriferids; square: Athyridids. Symbol colors indicate sedimentary facies: green: marly limestone; orange: marlstone; blue: limestone; yellow: clay rich marlstone. (A) Al/Ca (logarithmic scale) vs B/Ca. (B) Al/Ca (logarithmic scale) vs $\delta^{11}\text{B}$. (C) B/Ca vs $\delta^{11}\text{B}$. (D) Mg/Ca vs $\delta^{11}\text{B}$. (E) $\delta^{13}\text{C}$ vs $\delta^{11}\text{B}$. (F) $\delta^{18}\text{O}$ vs $\delta^{11}\text{B}$. (G) Sr/Ca vs Mn/Ca. Grey area represents the field of good preservation for brachiopod shells (Brand et al., 2003). (H) $^{87}\text{Sr}/^{86}\text{Sr}$ vs $\delta^{11}\text{B}$. (I) $\Delta^{87}\text{Sr}/^{86}\text{Sr}$ (expected – measured values) vs $\delta^{11}\text{B}$. (J) $^{87}\text{Sr}/^{86}\text{Sr}$ vs Sr/Ca.

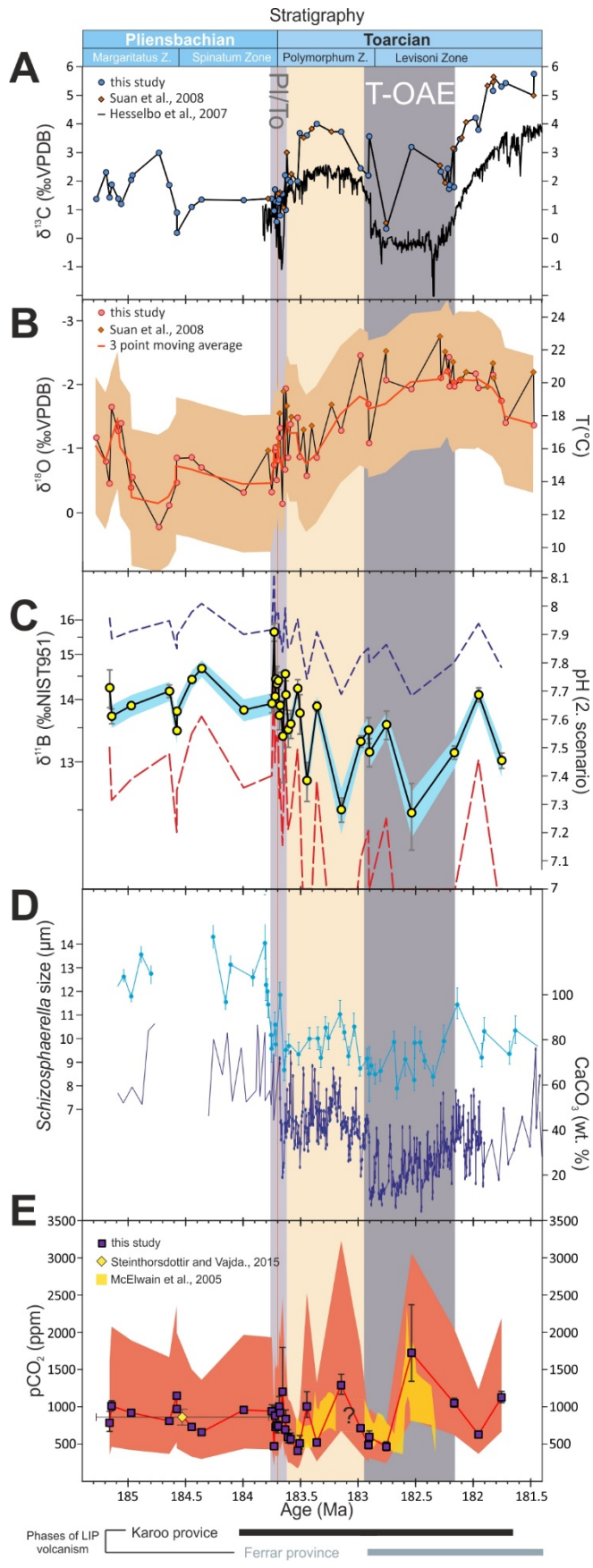


Figure S2. Alternative multi-proxy record across the Pliensbachian-Toarcian boundary (ammonite zone scale resolution), with seawater pH reconstructed following scenario 2 (inorganic borate ion incorporation into calcite (Klochko et al., 2006)). Pl/To—Pliensbachian-Toarcian boundary; T-OAE—Toarcian Oceanic Anoxic Event; Z.—Zone. (A) Bulk rock carbon isotope (black line; Hesselbo et al., 2007); brachiopod carbon isotope data (this study and Suan et al., 2008). VPDB—Vienna Peedee belemnite. (B) Brachiopod oxygen isotope and calibrated temperature record (this study and Suan et al., 2008); orange band: error envelope for temperature estimation, assuming seawater $\delta^{18}\text{O}$ of -2 to 0‰ (equivalent to salinity ± 2.5 ppt); (C) Boron isotope and calibrated pH record according to scenario 2 (Klochko et al., 2006); the blue band shows the propagated uncertainty based on analytical uncertainty for $\delta^{11}\text{B}$ ($\pm 0.2\%$ 2SD). Dashed lines mark the limits of pH envelope derived from the minimum and maximum pH of late Pliensbachian pH Neritan model of Ridgwell (2005). Plot is truncated at pH value 7, due to the fact that some values fell below the effective range of pH calibrations. NIST951—Boric acid isotopic standard. (D) Size of calcareous nannofossil *Schizosphaerella* (light blue) size and bulk rock CaCO_3 content (dark blue) (Suan et al., 2010). (E) $p\text{CO}_2$ records (published and new) with uncertainties (orange area, see Supplemental Material). Ages for the Karoo-Ferrar large igneous province after Ruebsam et al. (2019). “Z.”: Zone.

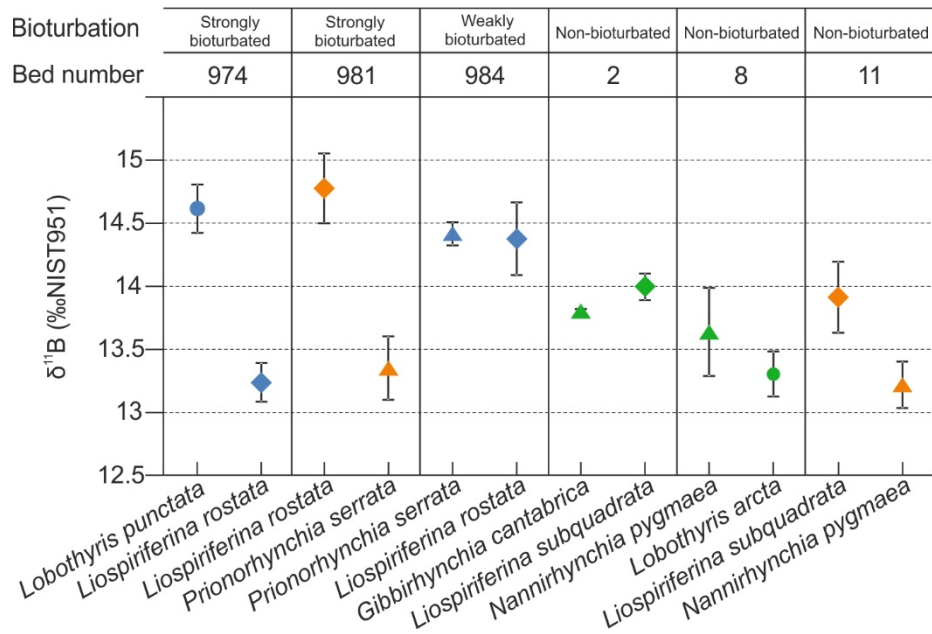


Figure S3. A comparison of $\delta^{11}\text{B}$ values across different brachiopod species from the same beds.

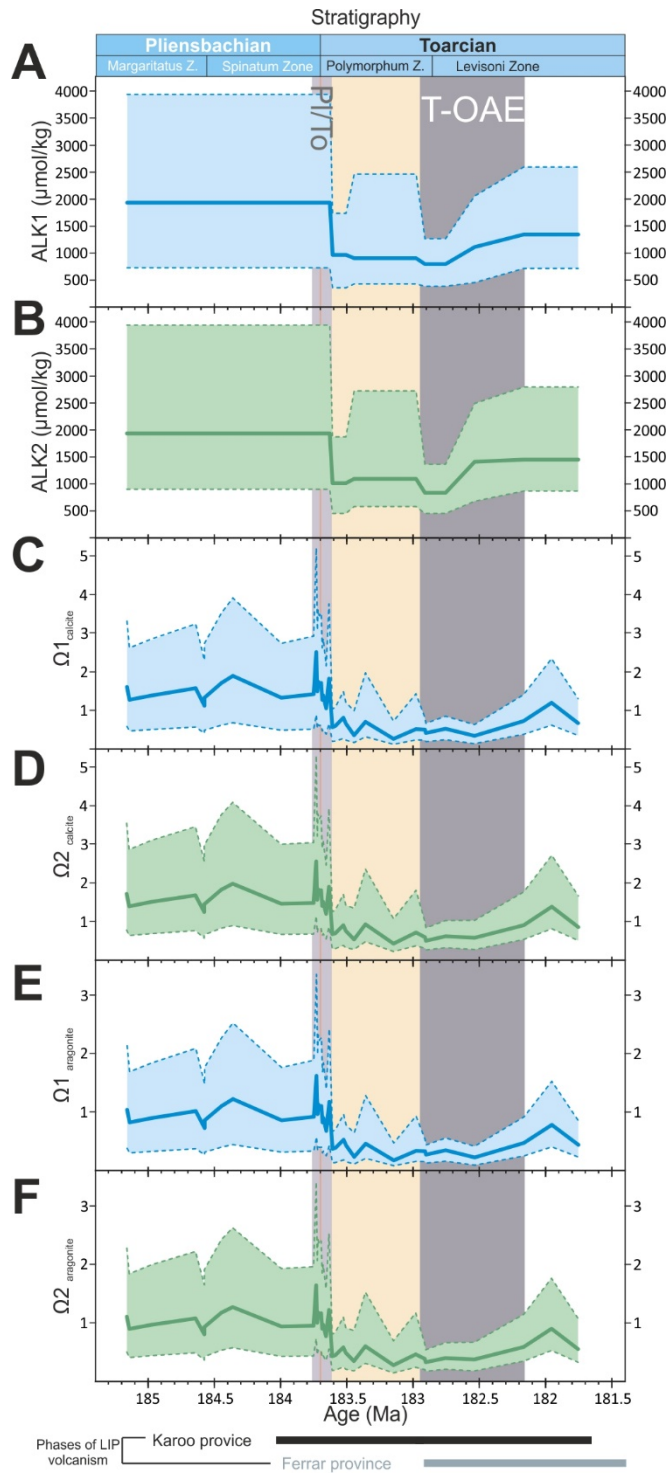


Figure S4. Modelled seawater alkalinity, aragonite and calcite saturation states over the late Pliensbachian and early Toarcian. (A) Alkalinity on the basis of pH scenario 1. (B) Alkalinity on the basis of pH scenario 2. (C) Calcite saturation according to pH scenario 1. (D) Calcite

saturation according to pH scenario 2. (E) Aragonite saturation according to pH scenario 1. (F) Aragonite saturation state according to seawater pH reconstructed from scenario 2.

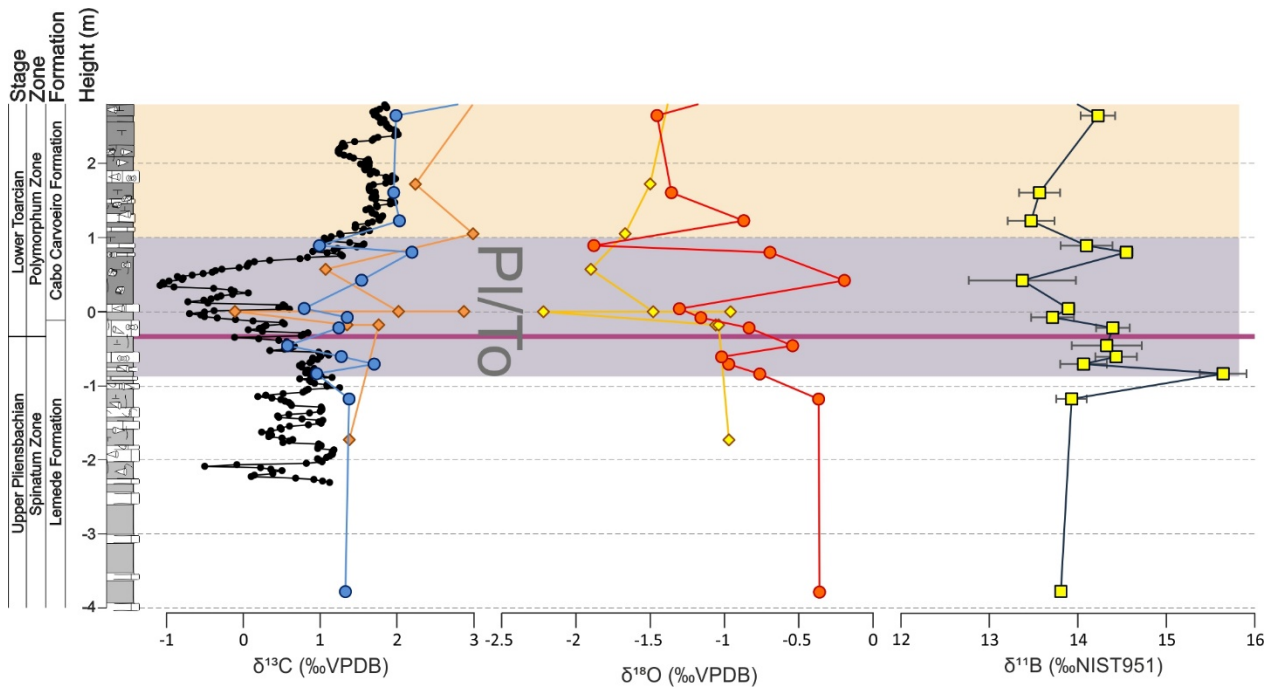


Figure S5. Enlarged carbon, oxygen and boron isotope record at the PI/To from Figure 1.

Stratigraphic log (after Hesselbo et al., 2007; modified by following Duarte et al., 2018) plotted against bulk $\delta^{13}\text{C}$ (Hesselbo et al., 2007), published (Suan et al., 2008) and new (this study) brachiopod $\delta^{13}\text{C}$, $\delta^{18}\text{O}$ data, and $\delta^{11}\text{B}$ data (error bars indicate 2SD on replicated analyses of each specimen).